Visualization of Propagation of Pulse Vibration along the Heart Wall and Imaging of its Propagation Speed

Hiroshi Kanai

Abstract— Though myocardial viscoelasticity is essential in the evaluation of heart diastolic properties, it has never been noninvasively measured in vivo. By the ultrasonic measurement of the myocardial motion, we have already found that some pulsive waves are spontaneously excited by aortic-valve closure (AVC) at end-systole (T_0) (IEEE UFFC-43(1996)791-810). Using a sparse sector scan, in which the beam directions are restricted to about 16, the pulsive waves were measured almost simultaneously at about 160 points set along the heart wall at a sufficiently high frame rate (UMB 27(2001)752-768). The consecutive spatial phase distributions clearly revealed wave propagation along the heart wall for the first time (IEEE UFFC-51(2005)1931-1942). The propagation time of the wave along the heart wall is very small and cannot be measured by conventional equipment. Based on this phenomenon, we developed a means to measure the myocardial viscoelasticity in vivo. The phase velocity of the wave is determined for each frequency component. By comparing the dispersion of the phase velocity with the theoretical one of the Lamb wave, which propagates along the viscoelastic plate (heart wall) immersed in blood, the instantaneous viscoelasticity is determined noninvasively (IEEE UFFC-51(2005)1931-1942). In this study, the phase distribution obtained by the sparse scan is interpolated and extrapolated, and then the spatial distribution of the instantaneous phase velocity of the wave components propagating from the base side to the apical side of the heart wall is obtained for the longitudinal cross-sectional image.

I. INTRODUCTION

For tissue characterization, shear waves are artificially actuated in tissues or phantoms to determine their propagation speed and viscoelasticity [1]–[7]. However, spontaneously actuated vibrations propagating in the heart wall, which differ from electrically excited waves [8]–[10], have not been recognized at all. This is understandable given that the actual wave which propagates along the heart wall is minute, namely, only several tenths of a millimeter, and that the delay time from the base to the apex of the heart is very small, only several milliseconds.

Conventional ultrasonography, computer tomography (CT), and magnetic resonant imaging (MRI) enable clinical visualization of cross-sectional images of the human heart, but their imaging is restricted to large motion (> 1 mm) and low frequency components (< 30 Hz). The tissue Doppler imaging (TDI) technique [11]–[16] enables determination of motion distribution of the myocardium in real time. Even in current measurement, however, the sampling frequency of the motion of the heart wall is low (at most 200 Hz [16]), that is, the sampling period is 5 ms, which is too long to detect the propagation time of the wave.

H. Kanai is with Graduate School of Engineering, Tohoku University, Sendai 980-8579, Japan `kanai@ecei.tohoku.ac.jp`
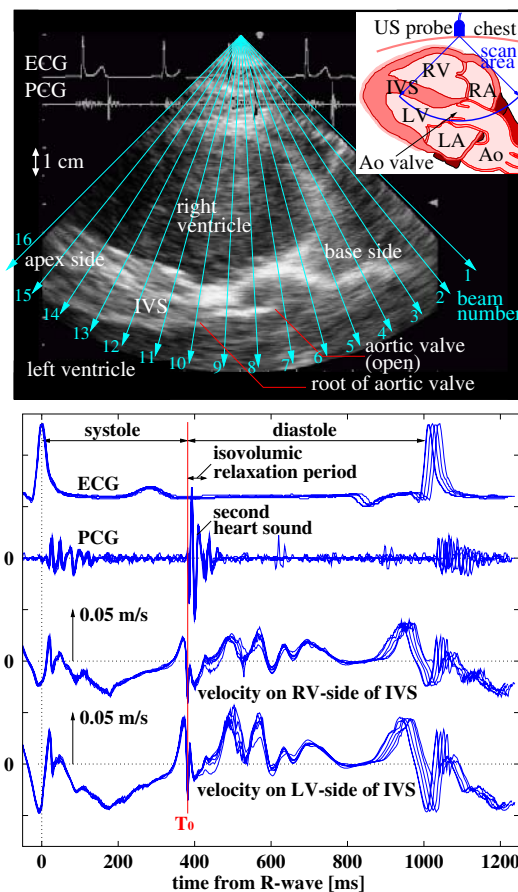

Fig. 1. upper: A cross-sectional image measured by conventional echocardiography in a healthy young male (subject A). The upper-right illustration shows the scanning range of the ultrasonic beams in this imaging. The arrows show the directions of the 16 ultrasonic beams used to measure the vibrations at about 160 points in the heart wall. lower: In vivo measurement results for the healthy man at two points set along the 13th ultrasonic beam. Each waveform for six consecutive cardiac cycles is overlaid.

We have previously developed an ultrasound-based transthoracic method (phased tracking method) to directly measure the heart wall vibrations [17]–[19]. RF pulses are transmitted from an ultrasonic transducer at a pulse repetition interval ΔT, and the reflected ultrasonic wave is received by the same transducer and quadrature-demodulated. The time-domain complex cross-correlation technique is applied to determine the phase shift between the consecutively obtained resultant signals. The phase shift corresponds to the displacement $\Delta x(t)$ during the short-period ΔT and the average velocity $v(t)=\Delta x(t)/\Delta T$ during that period. By accumulating the instantaneous displacement $\Delta x(t)$, the large motion $x(t)$ due to the heartbeat is tracked over one heartbeat, and at the same time, the minute vibration $v(t)$

superimposed on the large motion is obtained as a waveform. For this measurement, the sampling frequency (the time resolution) is increased from the 30 Hz in conventional echocardiography to 450 Hz to avoid aliasing. To realize this, the number of directions in which the ultrasonic beams are transmitted is greatly decreased from 240 to 16 as shown by the arrows in upper figure of Fig. 1(a).

We found that there is a steep dip in the pulse which occurs exactly at the time of AVC (T_0) [20], [21] as shown in lower figure of Fig. 1. This notch has been also measured by the TDI approach to determine the time of AVC (T_0) [22].

The use of the sparse sector scan [20] has allowed us to simultaneously measure heart-wall motion at 160 points at a sufficiently high frame rate to measure the propagation of the notch pulse along the interventricular septum (IVS). From consecutively obtained spatial distributions of the phase value of the vibration wave, our study [23] has revealed for the first time that the steep dip of the notch pulse propagates along the IVS from the base to the apex, and its phase velocity is determined. By analyzing various frequency components up to 90 Hz, the propagation speed shows the frequency dispersion.

We have shown that this dispersion characteristic agrees with the theoretical one of the Lamb wave which propagates in the viscoelastic plate immersed in fluid [23]. By introducing the single Voigt model into the equation of the Lamb wave and fitting the derived theoretical phase velocity to the measured dispersion, the myocardial viscoelastic properties are determined noninvasively for the first time [23].

In this paper, the instantaneous propagation speed of the pulse caused by the closure of the aortic valve is detected and its spatial distribution is visualized. The method is applied to human hearts and it is found that the propagation speed is not homogeneous in the heart wall.

II. PRINCIPLE

A. Spatial Distribution of the Instantaneous Phase of the Pulsive Vibration

Based on the method developed in [20], a spatial distribution of the instantaneous phase of the pulsive wave is obtained as shown in Fig. 2. The conventional cross-sectional image is shown in Fig. 3. In Fig. 2, the velocity signals as shown in Fig. 1 are measured at the multiple points set along the ultrasonic beam. The ultrasonic beams are scanned sparsely in 11 directions so that the aliasing does not occur and the time resolution is increased. Thus, the spatial distribution is coarse as shown in Fig. 2.

However, the wavelength of the propagating pulse wave is about 100 mm and the phase varies smoothly. Thus, interpolation and extrapolation can be applied to the phase distribution. The result is shown in Fig. 4.

B. Spatial Distribution of Instantaneous Speed of the Pulsive Vibration

Based on the definition of the phase velocity, the two spatial distributions $\theta(x; t-\Delta T)$ and $\theta(x; t)$ of the phase, which
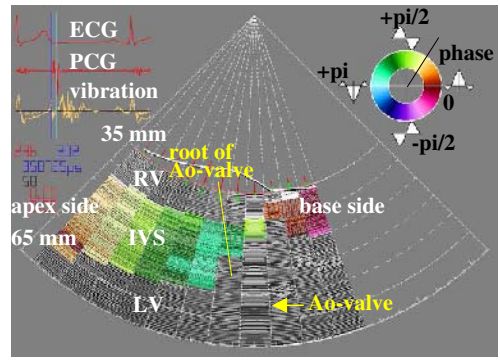

Fig. 2. Spatial distribution of color-coded phase values for 60-Hz component of the wavelets at a time of aortic valve closure without interpolation or extrapolation.
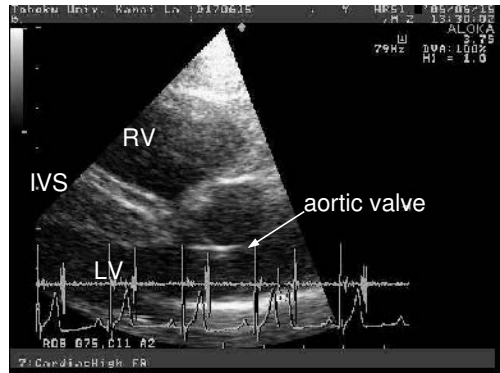

Fig. 3. B-mode cross-sectional image for the data in Fig. 2.

are obtained at the time interval of ΔT, are compared by the following complex cross-correlation function $R(\Delta x; x, t)$.

$$R(\Delta x; x, t) = \sum_{\delta x} \exp\{-j\theta(x + \Delta x + \delta x; t - \Delta T)\} \times \exp\{+j\theta(x + \delta x; t)\}, \qquad (1)$$

where Δx is the dislocation of the vibration during ΔT. By selecting Δx by which the angle $\angle R(\Delta x; x, t)$ becomes zero, the phase velocity at the point x in the myocardium at a time t is given by $c(x, t) = \Delta x/\Delta T$. The spatial distribution $c(x, t)$ of the instantaneous speed of the pulsive wave is shown in Fig. 5.
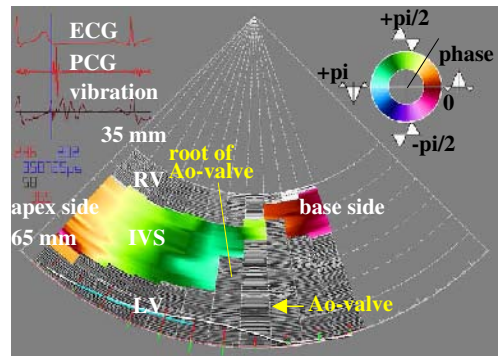

Fig. 4. Spatial distribution of color-coded phase values obtained by applying the spatial interpolation or extrapolation to that in Fig. 2 (for 60-Hz component, at a time of aortic valve closure).
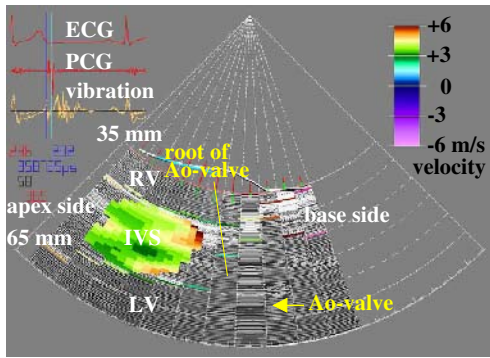
700

Fig. 5. Spatial distribution of instantaneous phase velocity $c(x,t)$ obtained for Fig. 4 (for 60-Hz component, at a time of aortic valve closure).
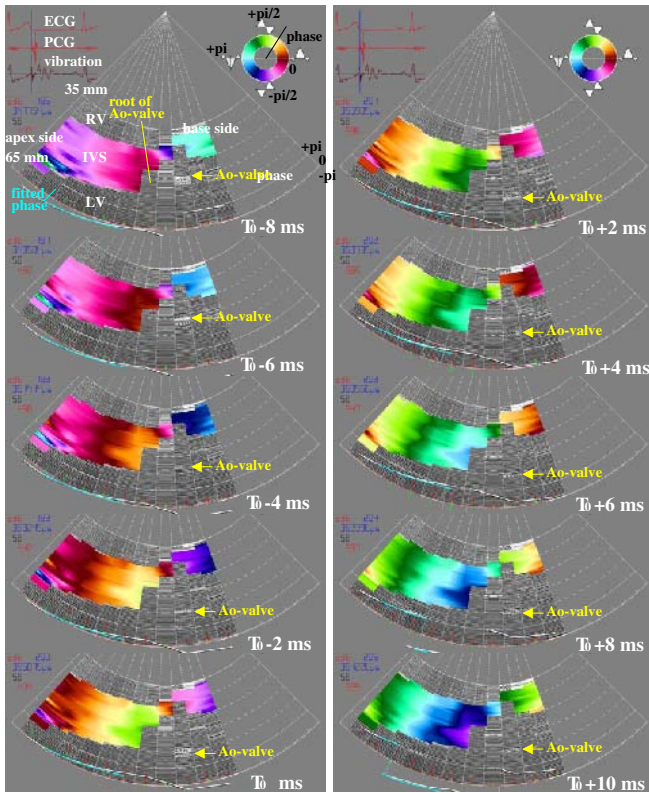

Fig. 6. Spatial distributions of color-coded phase value for 60 Hz component of the wavelet in Fig. 4. The spatial distributions are shown consecutively from T_0-8 ms to T_0+10 ms around the time of aortic valve closure (T_0).
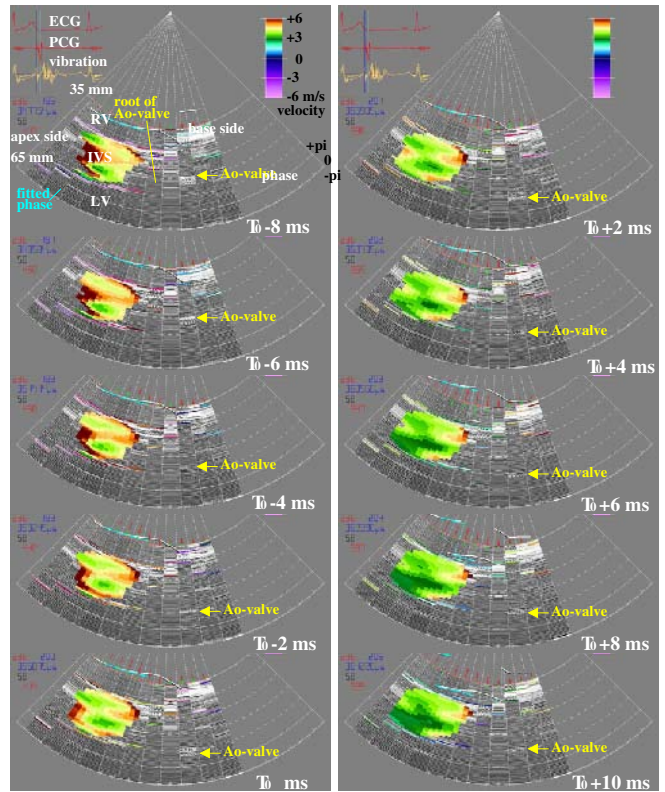

Fig. 7. Spatial distributions of regional velocity for 60 Hz component of the wavelet in Fig. 4. The spatial distributions are shown consecutively from T_0-8 ms to T_0+10 ms around the time of aortic valve closure (T_0).
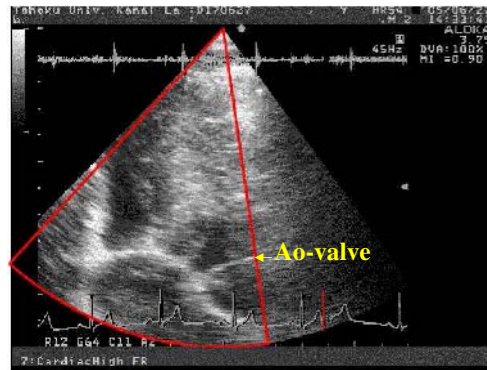

Fig. 8. Cross-sectional B-mode image of the IVS plane which is perpendicular to the conventional apical view for the subject in Fig. 7.

III. IN VIVO EXPERIMENTAL RESULTS

Figure 6 shows the spatial phase distributions with phase interpolation and extrapolation for the healthy subject in Figs. 2 and 4. Around the time of aortic valve closure (T_0), the spatial distributions are shown consecutively from T_0-8 ms to T_0+10 ms at every 2 ms. From the root of the aortic valve, the pulse vibration propagates from the base to the apical side.

Figure 7 shows the spatial distributions of the regional velocity regarding the phase distributions in Fig. 6. The phase velocity is almost constant for this 20 ms. However, the spatial distribution of the phase velocity is not homogeneous. The region which has larger phase velocity in the inter-

ventricular septum corresponds to the white region (fibrous region) in the conventional cross-sectional image in Fig. 3.

Figure 8 shows the cross-sectional B-mode image of the IVS plane which is perpendicular to the conventional apical view for the same subject.

Figure 9 shows the spatial distributions of the phase of the pulse vibration caused by the closure of the aortic valve. Around the time of aortic valve closure (T_0), the spatial distributions are shown consecutively from T_0-4 ms to T_0+12 ms. From these results, the pulse vibration detected in this study propagates from the root of the aortic valve to the apex along the plane of the interventricular septum.
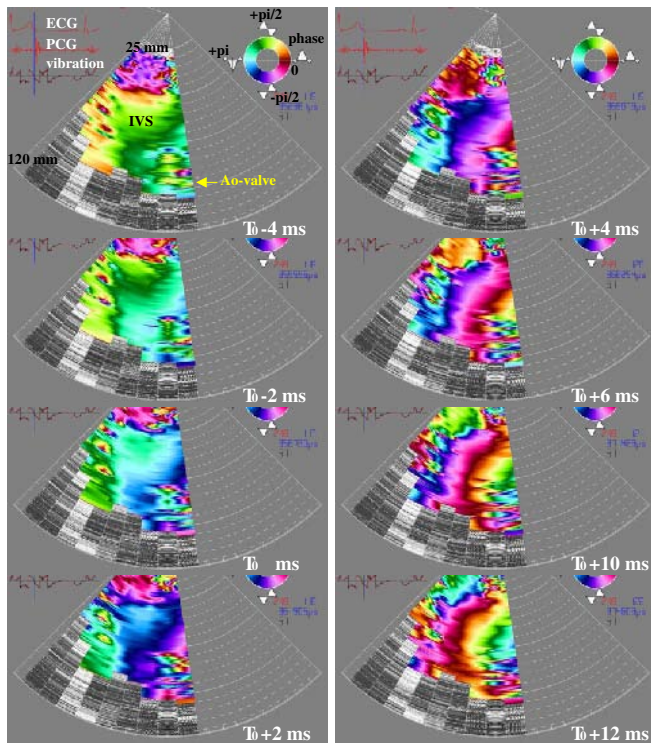
701

Fig. 9. Spatial distributions of color-coded phase value on the IVS plane which is perpendicular to the conventional apical view (for 60 Hz component of the wavelet for the subject in Fig. 8). The spatial distributions are shown consecutively from T_0-4 ms to T_0+12 ms around the time of aortic valve closure (T_0).

IV. CONCLUSIONS

We measured rapid and minute vibrations simultaneously at multiple points in the interventricular septum. Clear propagation of the pulsive wave along the interventricular septum was recognized. This method offers potential for in vivo imaging of the spatial distribution of the passive mechanical properties of the myocardium during the beginning of the isovolumic relaxation period, which would enable direct assessment of diastolic properties based on myocardial relaxation in heart failure.

ACKNOWLEDGMENTS

REFERENCES

[1] Y. Yamakoshi, J. Sato, and T. Sato, "Ultrasonic imaging of internal vibration of soft tissue under forced vibration," IEEE Trans. Ultrason., Ferroelect., Freq. Contr., vol. 37, no. 2, pp. 45-53, 1990.

[2] S. F. Levinson, M. Shinagawa, and T. Sato, "Sonoelastic determination of human skeletal muscle elasticity," J. Biomechanics, vol. 28, no. 10, pp. 1145-1153, 1995.

[3] S. Catheline, J-L. Thomas, F. Wu, and M. A. Fink, "Diffraction field of a low frequency vibrator in soft tissues using transient elastography," IEEE Trans. Ultrason., Ferroelect., Freq. Contr., vol. 46, no. 4, pp. 1013-1019, 1999.

[4] S. Catheline, F. Wu, and M. Fink, "A solution to diffraction biases in sonoelasticity: The acoustic impulse technique," J. Acoust. Soc. Am., vol. 105, no. 5, pp. 2941-2950, 1999.

[5] L. Sandrin, M. Tanter, J-L. Gennisson, S. Catheline, and M. Fink, "Shear elasticity probe for soft tissues with 1-D transient elastography," IEEE Trans. Ultrason., Ferroelect., Freq. Contr., vol. 49, no. 4, pp. 436-446, 2002.

[6] V. Dutt, R. R. Kinnick, and J. F. Greenleaf, "Acoustic shear wave displacement using ultrasound," 1996 IEEE Ultrason. Sympo. Proc., pp. 1185-1188, 1996.

[7] S. Chen, M. Fatemi, and J. F. Greenleaf, "Complex stiffness quantification using ultrasound stimulated vibrometry," 2003 IEEE Ultrason. Sympo. Proc., pp. 941-944, 2003.

[8] O. Anosov, S. Berdyshev, I. Khassanov, M. Schaldach, and B. Hensel, "Wave propagation in the atrial myocardium: Dispersion properties in the normal state and before fibrillation," IEEE Trans. Biomed. Eng., vol. 49, no. 12, pp. 1642-1645, 2002.

[9] S. P. Thomas, J. P. Kucera, L. Bircher-Lehmann, Y. Rudy, J. E. Saffitz, and A. G. Kléber, "Impulse propagation in synthetic strands of neonatal cardiac myocytes with genetically reduced levels of connexin43," Circ. Res., vol. 92, pp. 1209-1216, 2003.

[10] N. Sperelakis, "Origin of the cardial resting potential," in Handbook of Physiology. The Cardiovascular System. edited by R. M. Berne, N. Sperelakis, S. R. Geiger, American Physiological Society, Bethesda, MD, 1979. p. 190.

[11] G. R. Sutherland, M. J. Stewart, K. W. E. Groundstroem, C. M. Moran, A. Fleming, F. J. Guell-Peris, R. A. Riemersma, L. N. Fenn, K. A. A. Fox, and W. N. McDicken, "Color Doppler myocardial imaging: a new technique for the assessment of myocardial function," J. Am. Soc. Echocardiogr., vol. 7, pp. 441-458, 1994.

[12] A. Heimdal, A. Støylen, H. Torp, and T. Skjærpe, "Real-time strain rate imaging of the left ventricle by ultrasound," J. Am. Soc. Echocardiogr., vol. 11, pp. 1013-1019, 1998.

[13] K. Miyatake, M. Yamagushi, N. Tanaka, M. Uematsu, N. Yamazaki, Y. Mine, A. Sano, and M. Hirama, "New method for evaluating left ventricular wall motion by color-coded tissue Doppler imaging: in vitro and in vivo studies," J. Am. Coll. Cardiol., vol. 25, no. 3, pp. 717-724, 1995.

[14] P. Palka, A. Lange, A. D. Fleming, G. R. Sutherland, L. N. Fenn, and W. N. McDicken, "Doppler tissue imaging: myocardial wall motion velocities in normal subject," J. Am. Soc. Echocardiogr., vol. 8, pp. 659-668, 1995.

[15] J. Gorcsan III, V. K. Gulati, W. A. Mandarino, and W. E. Katz, "Color-coded measures of myocardial velocity throughout the cardiac cycle by tissue Doppler imaging to quantify regional left ventricular function," Am. Heart J., vol. 131, no. 6, pp. 1203-1213, 1996.

[16] G. R. Sutherland, G. D. Salvo, P. Claus, J. D'hooge, and B. Bijnens, "Strain and strain rate imaging: a new clinical approach to quantifying regional myocardial function," J. Am. Soc. Echocardiogr., vol. 17, no. 7, pp. 788-802, 2004.

[17] H. Kanai, M. Sato, Y. Koiwa, and N. Chubachi, "Transcutaneous measurement and spectrum analysis of heart wall vibrations," IEEE Trans. Ultrason., Ferroelect., Freq. Contr., vol. 43, no. 5, pp. 791-810, 1996.

[18] H. Kanai, H. Hasegawa, N. Chubachi, Y. Koiwa, and M. Tanaka, "Noninvasive evaluation of local myocardial thickening and its color-coded imaging," IEEE Trans. Ultrason., Ferroelect., Freq. Contr., vol. 44, no. 4, pp. 752-768, 1997.

[19] H. Kanai, Y. Koiwa, and J. Zhang, "Real-time measurements of local myocardium motion and arterial wall thickening," IEEE Trans. Ultrason., Ferroelect., Freq. Contr., vol. 46, no. 5, pp. 1229-1241, 1999.

[20] H. Kanai and Y. Koiwa, "Myocardial rapid velocity distribution," Ultrasound Med. Biol., vol. 27, no. 4, pp. 481-498, 2001.

[21] H. Kanai, S. Yonechi, I. Susukida, Y. Koiwa, H. Kamada, and M. Tanaka, "Onset of pulsatile waves in the heart walls at end-systole," Ultrasonics, vol. 38, no. 1, pp. 405-411, 2000.

[22] F. Jamal, T. Kukulski, J. Strotmann, M. Szilard, J. D'hooge, B. Bijnens, F. Rademakers, L. Hatle, I. D. Scheerder, and G. R. Sutherland, "Quantification of the spectrum of changes in regional myocardial function during acute ischemia in closed chest pigs: an ultrasonic strain rate and strain study," J. Am. Soc. Echocardiogr., vol. 14, no. 9, pp. 874-885, 2001.

[23] H. Kanai, "Propagation of Spontaneously Actuated Pulsive Vibration in Human Heart Wall and in vivo Viscoelasticity Estimation," IEEE Trans. Ultrason., Ferroelect., Freq. Contr., vol. 51, no. 11, pp. 1931-1942, 2005.